The ParTI array for studying pionic fusion

A. Zarrella, A. Bonasera, L. Heilborn, A. Jedele, A.B. McIntosh, and S.J. Yennello

Pionic fusion is the process by which two nuclei fuse during a collision and then deexcite by the exclusive emission of a pion. The resulting compound nucleus is left in or near its ground state [1]. The process requires that nearly all of the available kinetic and potential energy in the colliding system be concentrated into two degrees of freedom - the rest mass and kinetic energy of the emitted pion. Thus, the energy of the emitted pion is limited by the number of available final states of the fusion residue [2]. The combination of limited available energy and the extreme coherence required in the process ensures that the pionic fusion channel is greatly suppressed. Indeed, the measured pionic fusion cross sections range from hundreds of nanobarns for the lightest systems (He + He) to hundreds of picobarns as one moves to larger systems (A_{tot} = 6 - 24) [2-12].

During this past year we have continued making progress towards measuring pionic fusion cross sections using the Momentum Achromat Recoil Spectrometer (MARS) [13] and the newly constructed Partial Truncated Icosahedron (ParTI) phoswich array. In July of 2015, we ran an experiment in which we calibrated a representative phoswich detector using secondary beams at the back of MARS and developed a method for calibrating the ParTI array based on the results of this representative unit. In December of 2015, we performed the first test of a significantly populated (12 of the 15 total phoswich units) ParTI array in beam in order to develop a procedure for aligning the array and to see particle identification lines in all detectors. The most recent test run took place in February of 2016 and sought to test various aspects of the Pionic Fusion experiment and to attempt to identify pions using 4 ParTI phoswich detectors.

During the phoswich calibration test experiment in July of 2015, we were able to measure the phoswich detector response for Z = 1, 2, and 3 charged particles at known energies using secondary beams created by the reaction of $^{14}N + ^{9}Be$ at 40 MeV/u and the MARS. This information was used to correct the resulting ΔE-E particle identification plots and produce energy-calibrated data. Fig. 1a shows some raw ΔE-E data from that run which shows particle identification lines for charged particles through 6Li. The y-axis is the integration of the phoswich response inside of a “fast” gate encompassing the first approximately 50 ns of the signal. The x-axis is the integration of the phoswich response inside of a “slow” gate encompassing approximately 400 ns of the phoswich response separated from the end of the fast gate by 200 ns. Fig. 1b shows the corrected, energy-calibrated data from Fig. 1a. Now, the y-axis corresponds to the energy deposited in the fast plastic component of the phoswich and the x-axis corresponds to the energy deposited in the CsI component of the phoswich. Using Fig. 1b we have developed a method for energy calibrating the ParTI array using a similar technique as that reported in [14].

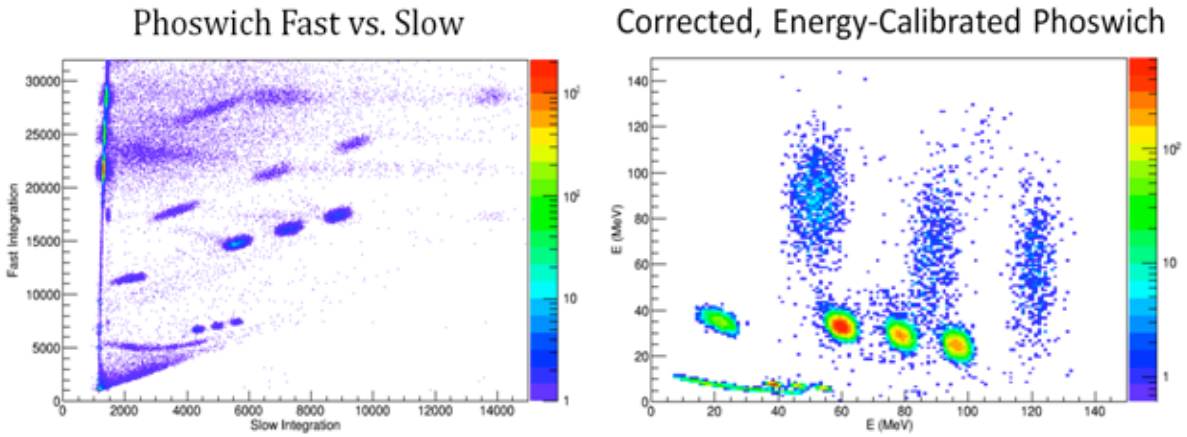

FIG. 1. a) Fast Integration vs. Slow Integration results for a representative phoswich using secondary beams produced by MARS. Moving from bottom to top, we can identify the particle lines: the positively sloped line at the bottom is the neutron/gamma line, above that is the proton line (4 poorly resolved proton energies) followed by 3 energies of deuterium, 1 energy of ^{3}He, 3 energies of alpha, 3 energies of ^{6}Li and, finally, a single energy of 10B. b) A ΔE-E plot representing data for Z = 1, 2, and 3 from a) after being corrected and energy calibrated.

In the test run performed in December of 2015, we confirmed that we were able to install and successfully align the populated ParTI array inside the MARS production chamber. A beam of 16O at 60 MeV/u was collided with a gold target and fragments were measured in the backward direction. Two representative fast vs. slow plots are shown in Fig. 2. As in Fig. 1a, the y-axis is the integration of the phoswich signal inside the fast gate and the x-axis is the integration of the signal inside the slow gate. The obtained particle identification was quite poor in this test experiment. The cause of this poor resolution was determined to be because of the construction of the PMT bias cables powering the detector array. The old ribbon cable design has since been replaced with an all coaxial cable design. This test run also alerted us to the need for further shielding of the ParTI array from beam halo and unwanted contamination accompanying the beam down the line and entering the phoswiches from the back. In response to this, we have added a tungsten alloy radiation shield behind the detector array.

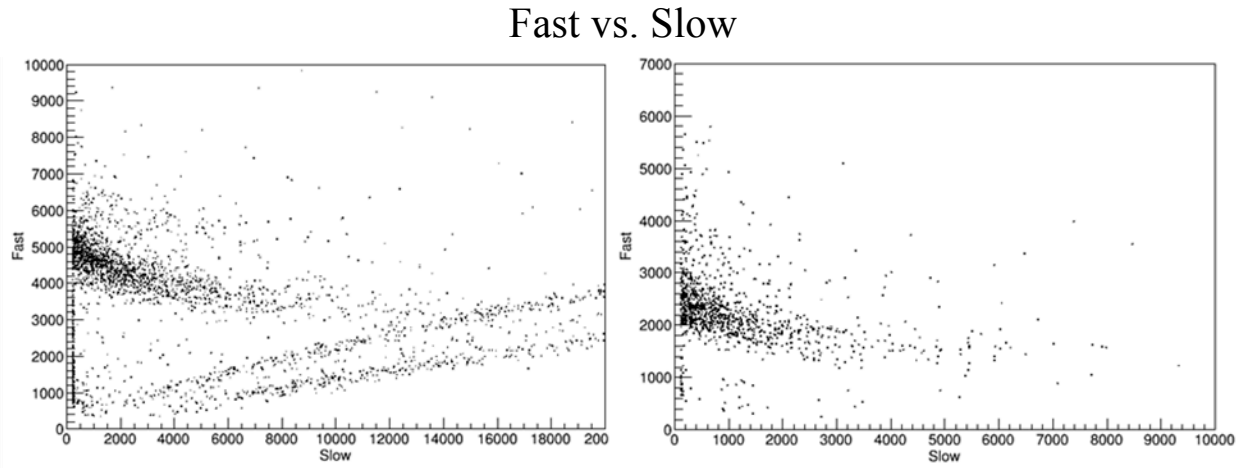

FIG. 2. Two fast vs. slow particle identification plots from two representative detectors from the test experiment in December of 2015. In both cases, we can see a prominent band representing Z = 1 particles with some counts above in each case which could potentially be the beginnings of a Z = 2 band. However, we have clearly lost resolution compared to Figure 1 as isotopic lines are not distinguishable in either case.

During the beam experiment in February of 2016 we used a beam of alpha particles at 55 MeV/u to diagnose quite a few aspects of our experimental plan. Firstly, an aluminum beam degrader was inserted into the line inside the K500 vault which slowed the beam down to approximately 46.5 MeV/u. This degraded beam was then able to be focused onto our target position with an intensity loss of approximately a factor of 10, an acceptable loss for performing the pionic fusion background measurement. Next, we were able to show that a newly inserted Faraday cup located inside the MARS D1 magnet was capable of registering a beam current for both the 55 MeV/u and degraded alpha beams. This cup will provide a continuous proportional measure of beam intensity during the pionic fusion production run. Lastly, 4 phoswich detectors were arranged inside the production chamber. In order to test the resolution of the phoswiches using the new coaxial cables and to measure traditionally produced pions, a gold target was inserted into the 55 MeV/u alpha beam and reaction products were measured. Figure 3 shows data from one of the detectors in this experiment. The fast vs. slow plot is similar to those in Figures 1a and 2. It is clear that we are getting much better energy resolution and, consequently, much clearer particle identification lines for Z = 1 particles. While this data has helped develop algorithms for identifying pions using their characteristic decay response inside the detectors, we were unable to definitively identify any pions in our data.

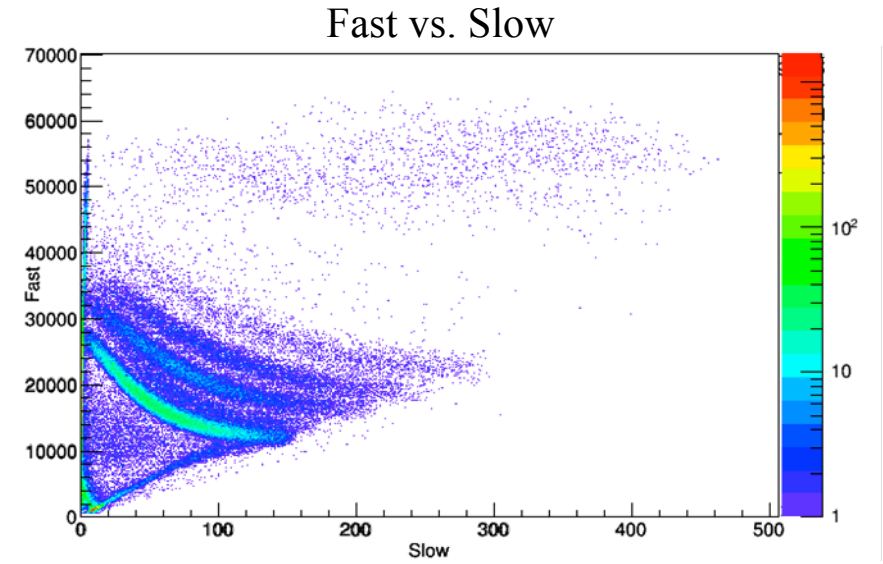

FIG. 3. A fast vs. slow particle identification plot produced by one of the detectors during the February 2016 test experiment. It is clear to see the better resolution as compared to the plots from figure 2. Here we see well separated particle identification for (moving up the plot) the neutron/gamma line, protons, deuterons, tritons and, at the very top, a band of Z = 2 particles. There is a somewhat weaker line located above the triton line and arriving at the y-axis at approximately 42,000, which corresponds to proton double hits.

In the summer of 2016, we plan to remeasure the transmission efficiency for our residues of interest through MARS and to run a second phoswich calibration experiment similar to the one from July of 2015. This second calibration experiment will reflect new electronics and measurement techniques that we have implemented over the last year. A pionic fusion production run is scheduled for next year.

[1] P. Braun-Munzinger and J. Stachel. Ann. Rev. Nucl. Part. Sci. **37**, 97 (1987).

[2] D. Horn, *et al*. Phys. Rev. Lett. **77**, 2408 (1996).
[3] Y. Le Bornec, *et al*. Phys. Rev. Lett. **47**, 1870 (1981).
[4] L. Joulaeizadeh, *et al.* Phys. Lett. B **694**, 310. (2011).
[5] W. Schott, *et al*. Phys. Rev. C **34**, 1406 (1986).
[6] M. Andersson, *et al.* Nucl. Phys. A **779**, 47 (2006).
[7] M. Andersson, *et al.* Phys. Lett. B **481**, 165 (2000).
[8] M. Andersson, *etal.* Phys. Scr. **T104**, 96 (2003).
[9] L. Bimbot, *et al.* Phys. Rev. C **30**, 739 (1984).
[10] L. Bimbot, *et al.* Phys. Lett. B **114**, 311 (1982).
[11] J. Homolka, *et al.* Phys. Rev. C **38**, 2686 (1988).
[12] N. Willis, *et al.* Phys. Lett. B **136**, 334 (1984).
[13] R.E. Tribble, *et al*. Nucl. Instrum. Methods Phys. Res. **A285**, 441 (1989).
[14] D.A. Cebra, *et al.* Nucl. Instrum. Methods Phys. Res. **A313**, 367 (1992).